

Optimal Design Emulators: A Point Process Approach

Matthew T. Pratola^{1,3}, C. Devon Lin^{2,4}, Peter F. Craigmile^{1,5}

¹ Department of Statistics, The Ohio State University, Columbus, OH 43210, USA

² Queen's University, Department of Mathematics and Statistics, Jeffery Hall, University
Avenue, Kingston, ON K7L 3N6, Canada

³mpratola@stat.osu.edu , ⁴devon.lin@queensu.ca , ⁵pfc@stat.osu.edu

Last updated December 14, 2024

Abstract

Design of experiments is a fundamental topic in applied statistics with a long history. Yet its application is often limited by the complexity and costliness of constructing experimental designs in the first place, which involve searching a high-dimensional input space and evaluating computationally expensive criterion functions. In this work, we introduce a novel approach to the challenging design problem. We will take a probabilistic view of the problem by representing the optimal design as being one element (or a subset of elements) of a probability space. Given a suitable distribution on this space, a generative point process can be specified from which stochastic design realizations can be drawn. The appropriate class of point processes is motivated by exploring a connection to Latin Hypercube designs. We then describe a scenario where the classical (point estimate) entropy-optimal design for Gaussian Process regression coincides with the mode of a particular point process. We conclude with outlining an algorithm for drawing such design realizations, its extension to sequential design, and

applying the techniques developed to constructing space-filling designs for Stochastic Gradient Descent and entropy designs for Gaussian process regression.

Keywords: Big data, Design of experiments, Determinantal point process, Exchange algorithm, Gaussian process, Stochastic gradient descent, Sequential design

1 Introduction

Optimal design of experiments (DOE) is a fundamental topic in statistics with a long history [e.g. [Fedorov, 1972](#), [Silvey, 1980](#), [Kiefer et al., 1985](#), [Atkinson et al., 2007](#), [Dean et al., 2017](#)]. Yet more recently, DOE has seemed to attract less attention from theoreticians, methodologists, and practitioners. One reason for this decreased interest may be due to an increased reliance on observational data, but this ignores current challenges in the statistical analysis of data. Datasets are becoming ever larger and more complex. Statistical models are more complicated than they once were. Uncertainty quantification is more challenging. As the challenges increase, DOE should play an important role in modern statistical analyses.

Typically DOE targets a particular aspect of a model which is deemed “important”, such as the prediction error in a spatial model, or the variance of some set of parameters of a regression model. Given n input settings $\boldsymbol{\xi}_1, \dots, \boldsymbol{\xi}_n$ drawn from some set $\chi \subset \mathbb{R}^d$, a design criterion $\mathcal{L}(\boldsymbol{\xi}_1, \dots, \boldsymbol{\xi}_n)$ is specified, and the n -run optimal design involves finding the input

settings Ξ_n that minimize this criterion:

$$\Xi_n = \arg \min_{\xi_1, \dots, \xi_n} \mathcal{L}(\xi_1, \dots, \xi_n). \quad (1)$$

In many settings, solving this problem is challenging. Assuming χ is a discretized candidate set of cardinality N , the number of possible designs to explore is $\binom{N}{n}$. The (Federov) *Exchange Algorithm* [Fedorov, 1972] is the most popular approach to solving this problem, which performs one-at-a-time updates to the design. Unfortunately, the optimization problem is notoriously difficult due to the large number of possible designs and the multi-modality of the optimization problem. More recently, modern optimization algorithms such as particle-swarm methods and simulated annealing [Chen et al., 2013] have been applied, but these can be difficult to implement reliably in modern settings [e.g. Nguyen et al., 2019].

When the dimensionality of the input space is high or the number of design points desired is large, performing optimal design remains practically infeasible. This is because constructing a designed experiment involves searching the d -dimensional input space $\chi \subset \mathbb{R}^d$, and, for each plausible solution, calculating an optimality criterion which can itself be computationally expensive. This challenging problem has typically only been made tractable by changing the optimality criterion to one based on a simplified model that is more computationally amenable. This approach is sometimes justifiable but rarely broadly desirable.

The goal of this work is to introduce a novel approach to the challenging problem of constructing optimal designs. Our focus in particular are designs for Gaussian process (GP)

regression models, which have broad applications in spatial statistics, computer experiments and statistical/machine learning [Sacks et al., 1989, Furrer et al., 2006, Cressie and Johannesson, 2008, Banerjee et al., 2008, Higdon et al., 2008, Guhaniyogi et al., 2011, Sang et al., 2011, Katzfuss, 2013, Pratola et al., 2013, 2014, Gramacy and Apley, 2015, Katzfuss and Hammerling, 2017]. We take a probabilistic view of the problem that is more general than the traditional probabilistic view previously discussed in the DOE literature [Kiefer et al., 1985, Müller, 2007]. The idea is to represent the collection of points that form an optimal design as being one element (or a subset of isometrically equivalent elements) of a stochastic process defined on the space of point patterns. By specifying an appropriate **generative point process** (PP) for this distribution, we introduce the idea of an *optimal design emulator*, where the classical optimal design solution typically coincides with the mode of this generative stochastic process. Since the generative process can be specified in terms of a low-dimensional parameter space, constructing an optimal design reduces to drawing a realization of this process given appropriately tuned parameter settings of the process rather than performing a difficult optimization problem. Among other things, this approach lends itself to a wide selection of Markov Chain Monte Carlo (MCMC) tools for efficient computation, and also gives a measure of how optimal the design drawn actually is. As such, our work draws a connection between PP models and optimal designs – particularly for Gaussian processes – while taking a distinctively Bayesian perspective on the design problem.

1.1 GP Regression and Design

The Gaussian process (GP) regression model is used extensively in modern applications as a model of an unknown, potentially smoothly varying, process $f(\mathbf{x})$, observed at continuous inputs $\mathbf{x} \in \mathbb{R}^d$. The continuous inputs \mathbf{x} represents the input settings where our process may be observed and/or predicted. In contrast, the discrete, countable, set of *design candidates* is represented as $\chi \subset \mathbb{R}^d$, from which n -run experimental designs $\Xi_n = \{\xi_1, \dots, \xi_n\}$ may be constructed, where $\xi_i \in \chi$, $i = 1, \dots, n$. The process $f(\mathbf{x})$ may or may not be observed with noise $\epsilon(\mathbf{x})$, leading to a model for the observations $y(\mathbf{x})$, given by

$$y(\mathbf{x}) = f(\mathbf{x}) + \epsilon(\mathbf{x}).$$

The error term $\epsilon(\mathbf{x})$ is often assumed to be independent and identically distributed (i.i.d.) normal with mean zero and error variance σ_ϵ^2 . In the simplest case, the unknown process $f(\mathbf{x})$ is modeled as a stationary GP with mean $E[f(\mathbf{x})] = \mu(\mathbf{x})$ and covariance $\text{Cov}(f(\mathbf{x}), f(\mathbf{x}')) = \sigma^2 c(\mathbf{x}, \mathbf{x}')$ at input settings $\mathbf{x}, \mathbf{x}' \in \mathbb{R}^d$ with mean model $\mu(\mathbf{x})$, process scale σ^2 , and positive definite correlation function $c(\mathbf{x}, \mathbf{x}')$. The choice of mean function can be as simple as a constant or can include covariates that are related to f . The popular choice of an isotropic Gaussian correlation function [Stein, 2012],

$$c(\mathbf{x}, \mathbf{x}') = \rho^{||\mathbf{x}-\mathbf{x}'||^2},$$

assumes a smooth, continuous, and infinitely differentiable response, where ρ is the correlation parameter of the GP. Given n observations $\mathbf{Y} = (y(\mathbf{x}_1), \dots, y(\mathbf{x}_n))$, and assuming $\mu(\mathbf{x}) = 0$ for all \mathbf{x} , the GP model is

$$\mathbf{Y} | \sigma^2, \rho \sim N_n(\mathbf{0}, \sigma^2 \mathbf{R} + \sigma_\epsilon^2 \mathbf{I}), \quad (2)$$

where $\mathbf{R}_{ij} = c(\mathbf{x}_i, \mathbf{x}_j)$ is the (i, j) entry of the correlation matrix \mathbf{R} .

In the setting of spatial statistics or computer experiments, the two most popular model-based design criteria are the *integrated mean squared prediction error (IMSPE) optimal designs*, $\mathcal{L} = \int_{\mathbf{x}} (Y(\mathbf{x}) - E[Y(\mathbf{x}) | \boldsymbol{\xi}_1, \dots, \boldsymbol{\xi}_n])^2 d\mathbf{x}$ and the *entropy optimal designs*, $\mathcal{L} = E[\log(f_{\mathbf{Y}})]$ where $f_{\mathbf{Y}}$ is the usual multivariate Gaussian density corresponding to (2). IMSPE optimal designs are useful as they minimize the error in out-of-sample predictions. Entropy optimal designs provide improved estimates of the GP correlation parameter, ρ , which can be important for accurately quantifying prediction uncertainties, interpreting which variables are active in a variable selection problem [Morris et al., 1993, Linkletter et al., 2006], or improved estimation of the variogram [Cressie, 1993].

Both the IMSPE and entropy-based criteria involve $\mathcal{O}(n^3)$ operations on the potentially large $n \times n$ correlation matrix \mathbf{R} , which makes an already challenging optimization problem even more difficult. An alternative approach is to use model-robust designs that are geometrically motivated, such as the Latin Hypercube Sampling (LHS) designs [McKay et al., 1979], or other space-filling designs such as maximin distance designs [Nychka et al., 2015, Carnell,

2016]. LHS designs are popular model-free designs that are colloquially described as “space-filling” designs, and are theoretically justified as variance-reduction designs [McKay et al., 1979] while also having theoretical connections to Gaussian Process (GP) regression models [Johnson et al., 1990]. Maximin distance designs were found to be the limiting form of entropy optimal designs for GP regression as the correlation ρ decays to 0 [Johnson et al., 1990]. Similar to LHS and maximin designs, both IMSPE and entropy designs empirically lead to designs exhibiting “space-fillingness”, that is the chosen design points tend to spread out over the design region thereby filling-in any empty space, such as the LHS sample shown in Figure 1(c). However, LHS and maximin designs are usually more amenable in terms of computational cost. In practice, a combined criterion is often used, such as the space-filling LHS implemented in the popular R package `fields` [Nychka et al., 2015].

1.2 Point Patterns

The statistical study of *point patterns* attempts to classify what type of pattern a given, observed, set of points exhibits. Such applications are numerous in the area of ecology where often the spatial location and spatial density of an object being studied is to be inferred and possibly also used for prediction. For example, the location of trees in a forest form a geographically indexed set of points and the pattern exhibited by these points relate to the competition for resources between trees in a given forest, while such patterns of competition may also differ between species of trees.

A common summary measure of such point patterns are the nearest-neighbour distribution

functions $F(h)$ and $G(h)$ [Diggle, 2006] defined as functions of distance, h , where $F(h)$ denotes the probability a point has nearest grid neighbour less than h units away and $G(h)$ denotes the probability a point has a nearest neighbour point less than h units away. These measures can be used to categorize point patterns as follows:

$$F(h) > G(h) \Rightarrow \text{regular point pattern;}$$

$$F(h) = G(h) \Rightarrow \text{complete spatial randomness;}$$

$$F(h) < G(h) \Rightarrow \text{clustered point pattern.}$$

These classification rules make intuitive sense. For instance, imagine a 2-dimensional space over which we overlay a regular grid, and for simplicity let us assume the grid spacing is 1 unit in size. For fixed h , when $F(h)$ is large it means there is a high probability that one would observe a point $\leq h$ units from the nearest grid intersection. Similarly, for fixed h , when $G(h)$ is large it means there is a high probability that one would observe a point $\leq h$ units from another point in the point pattern. So, when $F(h)$ dominates $G(h)$ for all h , it means points have a higher probability of being near a grid intersection than another point at all distances h , hence the notion of a ‘regular’ point pattern. Meanwhile, if $G(h)$ dominates $F(h)$ at all distances h , it means points have a higher probability of being near one another rather than being near a grid intersection, hence the notion of a ‘clustered’ point pattern. When both of these functions are approximately equal, then we have ‘complete spatial randomness’ – the pattern of points realized have no discernable pattern at all.

To visualize this classification of point patterns, we consider 3 scenarios: point patterns

generated uniformly at random, point patterns generated to exhibit clustering, and point patterns generated as LHS designs using the R package `lhs` [Carnell, 2016]. All three examples were investigated in $p = 2$ dimensions with each pattern consisting of $n = 20$ points, and for each of these point patterns, we calculated empirical estimates of the functions F and G along with the empirical 95% pointwise confidence intervals over 1,000 replicates. Figure 1(a-c) displays sample draws of the random, clustered, and LHS point patterns. The corresponding mean and associated pointwise confidence intervals for the F and G functions are shown in Figure 1(d-f). From this figure, one would reasonably conclude that $F(h) > G(h)$ for the point patterns generated as LHS designs. This suggests that space-filling designs belong to the class of regular point patterns rather than clustering, or random, point patterns. This recognition – interpreting the patterns of design points from the perspective of statistical models for point patterns – will lead to our proposal for a probabilistic emulator of optimal designs for GP regression.

1.3 Point Processes

Let $\Xi = \{\xi_1, \dots, \xi_n\}$ represent a point pattern of cardinality n and let $Z(\mathbf{x})$ represent a stochastic point process defined on all $\mathbf{x} \in \mathbb{R}^d$. Such a process assigns a probability measure $\mathcal{F}_Z : \Xi \subseteq \mathcal{D} \rightarrow [0, 1]$, where $\mathcal{D} \subset \mathbb{R}^d$ could be a continuous subset of \mathbb{R}^d , or some discrete, countable subset of cardinality $|\mathcal{D}| = N$. In the former interpretation, the **point process** (PP) can be viewed as assigning the probability that a point will be realized in some infinitesimal region $d\mathbf{x}$ about \mathbf{x} . In the latter interpretation, one can view the PP realization

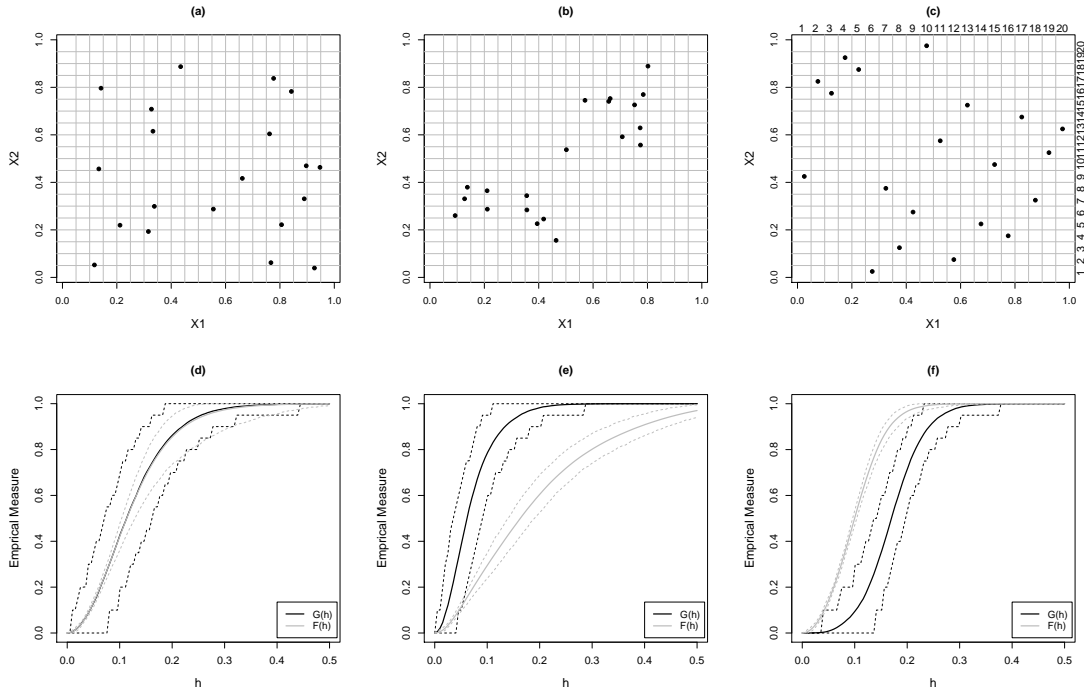


Figure 1: (a) Random point pattern generated by drawing from the uniform distribution. (b) Clustered point pattern generated by drawing from the Normal distribution with mean 0.5 and standard deviation of 0.125. (c) A sample LHS with 20 bins per dimension. In practice, the design point is taken at the centroid of each bin or uniformly drawn within each bin. (d) Estimates of nearest-neighbor distribution functions, $F(h)$ and $G(h)$, with 90% pointwise confidence intervals from 1,000 replicates of random designs. (e) Estimates of nearest-neighbor distribution functions, $F(h)$ and $G(h)$, with 90% pointwise confidence intervals from 1,000 replicates of clustered designs. (f) Estimates of nearest-neighbor distribution functions, $F(h)$ and $G(h)$, with 90% pointwise confidence intervals from 1,000 replicates of LHS space-filling designs.

as an N -vector such that n entries take the value 1, indicating presence of some element $\xi \in \mathcal{D}$ in the point pattern, and $N - n$ entries taking the value 0 indicating absence. In either setting, the point pattern is described by the number, n , of points making up the realization, and the location of these points, here denoted by the $\Xi = \{\xi_1, \dots, \xi_n\}$ [Geyer and Møller, 1994, Diggle, 2006, Lavancier and Møller, 2015].

Typical applications of PP modeling are in spatial statistics [e.g. Diggle, 2006] where the

locations are coordinates in a subregion of \mathbb{R}^2 , but we consider more generally the location of points in a subregion of \mathbb{R}^d . We assume simple PP models, that is at any given location \mathbf{x} we will only ever realize at most one point at \mathbf{x} . We also assume stationary PP models throughout, although this is not necessary in general. The simplest PP model is the Poisson [e.g. Daley and Vere-Jones, 2003], where the probability of a point in the domain \mathcal{D} belonging to the point pattern is given by the Poisson distribution with rate parameter given by the *first order intensity function*, λ_Z , defined as

$$\lambda_Z(\mathbf{x}) = \lim_{|d\mathbf{x}| \rightarrow 0} \frac{E(Z(d\mathbf{x}))}{|d\mathbf{x}|},$$

which implies the average number of points one expects to be generated within an arbitrary subregion of \mathcal{D} under the Poisson assumption. Furthermore, due to the memoryless property of the Poisson model, the existence of a point in some arbitrary Borel-measurable subregion B of \mathcal{D} is independent of the existence of a point in some arbitrary Borel-measurable subregion B' of \mathcal{D} . For this reason, the Poisson model is referred to as a point process model of complete spatial randomness.

Besides the complete random point patterns of the Poisson model, we have already seen that there are two additional possibilities: *clustered point patterns* and *regular point patterns*. These cases will necessarily require additional parameterization to capture the form of non-independence of points that give rise to clustered or regular point patterns. The straightforward extension of the intensity function formulation of the Poisson model is to introduce the so-called *second order intensity function*, $\lambda_{2,Z}$, defined as

$$\lambda_{2,Z}(\mathbf{x}, \mathbf{x}') = \lim_{|\mathbf{dx}| \rightarrow 0, |\mathbf{dx}'| \rightarrow 0} \frac{E(Z(\mathbf{dx})Z(\mathbf{dx}'))}{|\mathbf{dx}||\mathbf{dx}'|}.$$

The second-order intensity function simply captures the expected number of points that will jointly co-occur in infinitesimal regions about \mathbf{x} and \mathbf{x}' . One can also classify the type of PP using these intensity functions and the first order intensities by essentially considering the covariance properties of the process [Diggle, 2006]:

$$\begin{aligned} \lambda_{2,Z}(\mathbf{x}, \mathbf{x}') < \lambda_Z(\mathbf{x})\lambda_Z(\mathbf{x}') &\Rightarrow \text{regular point pattern,} \\ \lambda_{2,Z}(\mathbf{x}, \mathbf{x}') = \lambda_Z(\mathbf{x})\lambda_Z(\mathbf{x}') &\Rightarrow \text{complete spatial randomness,} \\ \lambda_{2,Z}(\mathbf{x}, \mathbf{x}') > \lambda_Z(\mathbf{x})\lambda_Z(\mathbf{x}') &\Rightarrow \text{clustered point pattern.} \end{aligned}$$

That is, a positive covariance $C_Z(\mathbf{x}, \mathbf{x}') = \lambda_{2,Z}(\mathbf{x}, \mathbf{x}') - \lambda_Z(\mathbf{x})\lambda_Z(\mathbf{x}')$ indicates that it is relatively more likely for points to co-occur than under the Poisson model, which generates clustered point patterns. Similarly, a negative covariance indicates that it is relatively less likely for points to co-occur than under the Poisson model, which generates regular point patterns.

In Section 2 we will explore the properties of space-filling (LHS) designs from the perspective of point processes (PPs). As alluded to above, the PP models that interest us are those that generate point patterns that fall in the regular class. In fact, we will establish theoretical connections between PPs and LHS designs via the intensity functions defined above, and then motivate the appropriate class of PP model for GP entropy designs. In Section 3 we introduce a particular regular point process model, the *determinantal point processes* (DPPs)

[Lavancier et al., 2015], and show how these repulsive point process models are connected to the stationary GP model outlined in Section 1.1. We then introduce the concept of a *design emulator* – a PP model that assigns a probability measure to the space of possible design point patterns such that the classical optimal design coincides with the mode – and devise an efficient algorithm that can be used to sample entropy optimal designs for GPs from the emulator. Section 4 explores examples of our design emulator applied to the popular stochastic gradient descent algorithm and for sequential GP regression. We conclude in Section 5. All proofs of results are presented in the Appendix.

2 Point Processes and Optimal Designs

We start by exploring the point process connection to LHS designs more deeply before moving on to focus specifically on the GP regression scenario.

2.1 Latin Hypercube Sampling Designs and Point Processes

LHS designs [McKay et al., 1979] are geometrically motivated to select design points that spread out over the design region of interest. They are popular due to their simple construction: for an n -run design in p dimensions, split each dimension into n bins and assign a random permutation of the bin indices $1, \dots, n$ to each column of the design matrix such that no row contains the same bin index more than once. A design constructed according to this simple algorithm is an LHS. An example LHS is shown in Figure 1(c) where the bin

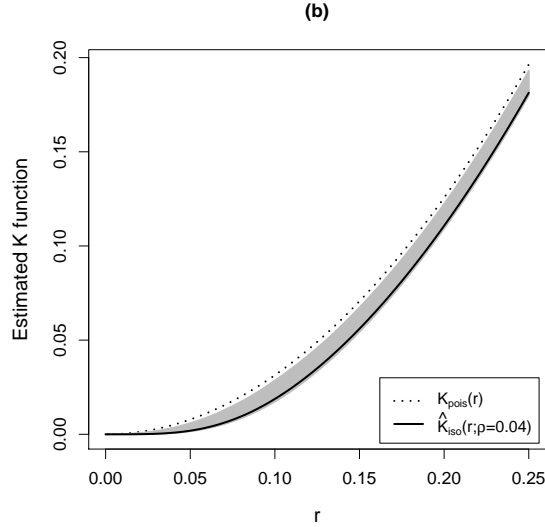


Figure 2: Estimated Ripley’s K function, \hat{K}_{iso} , taken as the pointwise median with corresponding 90% uncertainty interval (shown in grey) from 1,000 replicates of estimated entropy-optimal designs (dotted line represents Ripley’s function under random sampling, K_{pois} , for comparison).

labels have been noted on the top and right axes, and it is evident that LHS designs tend to spread-out over the design region of interest rather than exhibiting a clustering pattern. In practice, the actual design point might be taken as the centroid of each bin or a uniformly generated location within each bin, but the bin arrangement is the key part of the procedure. Given this construction of LHS designs, a direct connection between PPs and LHS designs can be established using the intensity function definitions described in Section 1.3, as summarized in Theorem 1.

Theorem 1. LHS designs belong to the class of simple, regular PPs satisfying $\lambda_{2,Z}(\mathbf{x}, \mathbf{x}') < \lambda_Z(\mathbf{x})\lambda_Z(\mathbf{x}')$ for any $\mathbf{x}, \mathbf{x}' \in \mathbb{R}^d$.

Thus, Theorem 1 shows that LHS designs belong to the class of regular PPs. The proof, given in the appendix, follows using a counting argument. In practice, the LHS design construction algorithm outlined above is augmented by a space-filling criterion. The idea of the augmented criterion is to select the “best” (in terms of space-fillingness) possible LHS design amongst all possible LHS designs. Since space-filling LHS designs are a subset of LHS designs in general, Theorem 1 implies that such constrained space-filling designs also fall in the class of regular PPs.

A deeper connection between the class to which point patterns belong (e.g. random, clustered or regular), and the corresponding intensity functions of the PP, can be established via the concept of negative quadrant dependence [Lehmann, 1966].

Lemma 1. [Lehmann] Two random variables, X and X' are said to be *negative quadrant dependent* (NQD) if $P(X \leq x, X' \leq x') \leq P(X \leq x)P(X' \leq x')$. Furthermore, let $U = r(X_1, \dots, X_d)$ and $V = s(X'_1, \dots, X'_d)$ for independent pairs of random variables $(X_i, X'_i), i = 1, \dots, d$. Then U, V are NQD if, for each i , X_i, X'_i are NQD and r, s are concordant functions in the i th coordinate.

Here, concordant functions are functions which are either both monotone increasing or monotone decreasing in a single argument when holding the remaining arguments fixed. Now, let us extend the definition of NQD to a design as follows.

Definition. Let $\Xi_n = \{\mathbf{X}_1, \dots, \mathbf{X}_n\}$ be a design with $\mathbf{X}_i = (X_{i1}, \dots, X_{id})$. If X_{ij}, X_{ik} are NQD for all $j \neq k$ and all $i \in 1, \dots, n$, then we say Ξ_n is an NQD design.

Based on this definition and Lemma 1, we have the following theorem that shows that designs falling in the class of regular PPs are necessarily NQD designs.

Theorem 2. Let Ξ_n be a design with design points $\mathbf{X}_i = (X_{i1}, \dots, X_{id})$ generated from a regular PP and suppose (X_{ik}, X_{jk}) are pairwise independent for all $i \neq j$. Then Ξ_n is an NQD design.

The proof of Theorem 2 relies on the definition of the intensity function as the expectation of the Bernoulli random variable $Z(d\mathbf{x})$ along with Lemma 1. A lemma of Hoeffding [Lehmann, 1966] extends the necessary condition to negative covariance.

Lemma 2. [Hoeffding] Let F denote the joint distribution of U, V and F_U, F_V denote the marginal distributions of U, V respectively. Then $Cov(U, V) = \int_{-\infty}^{\infty} \int_{-\infty}^{\infty} [F(u, v) - F_U(u)F_V(v)]dudv$.

From Lemma 2 and Lemma 1, we immediately see that NQD implies negative covariance for pairs of input settings. Combined with the assumption of concordant functions, these results imply that designs falling in the class of regular PPs exhibit negative covariance among the selected design points. This interpretation in fact coincides with McKay et al. [1979] original motivation, and subsequent proof, for LHS designs being superior from the perspective of reducing the variance of estimators. In particular, for estimators of the form $T = \sum_{i=1}^n g(Y_i)$ where $Y_i = h(X_{i1}, \dots, X_{id})$ is assumed to be monotonic in each of its arguments, the designed inputs, McKay et al. [1979] shows LHS designs have less variability than uniform random designs for such estimators; i.e., $\text{Var}(T_L) \leq \text{Var}(T_R)$, where T_L is the estimator T calculated using an LHS design while T_R refers to T calculated using random

sampling (a uniform random sample from the underlying distribution of input variables). In their proof, the variance reduction is due to a negative covariance term that arises from a monotone function of the design points. Theorem 2 more broadly captures this idea and connects it to the regular PP class, albeit showing that in general we only have a necessary condition for being in the regular class.

Besides the general motivation of LHS designs as a variance-reduction technique for functionals of designs points, LHS designs are also popular in GP regression [Johnson et al., 1990], which suggests that optimal designs for GP regression also lie in the class of regular PPs. By considering entropy optimal designs for GPs, we obtain a more direct connection to PPs, as we now demonstrate.

2.2 GP Entropy Optimal Designs and Point Processes

Let us consider the simplest case of our GP regression model defined in Section 1.1, with a mean trend of $\mu(\mathbf{x}) = 0$ and noise-free observations, i.e. $\sigma_\epsilon^2 = 0$. The GP model in this case is commonly used in computer experiments and in spatial statistics where a “nugget” term is not required. In this setting, the entropy optimal criterion for an n -run design, $\boldsymbol{\xi}_1, \dots, \boldsymbol{\xi}_n$, drawn from the discrete candidate set $\chi \subset \mathbb{R}^d$ can be shown to reduce to [Shewry and Wynn, 1987]

$$\mathcal{L}(\boldsymbol{\xi}_1, \dots, \boldsymbol{\xi}_n) = -\det(\mathbf{R}), \tag{3}$$

where the $n \times n$ correlation matrix \mathbf{R} has entries $\mathbf{R}_{ij} = c(\boldsymbol{\xi}_i, \boldsymbol{\xi}_j)$. [Johnson et al. \[1990\]](#), [Morris et al. \[1993\]](#), [Mitchell et al. \[1994\]](#) established that entropy optimal designs for GPs are asymptotically equivalent to maximin designs as the correlation becomes weaker, i.e. as $\rho \rightarrow 0$ in the correlation function $c(\boldsymbol{\xi}, \boldsymbol{\xi}')$. This is a convenient result as typically the correlation parameter ρ is not known a-priori. This asymptotic result provides a justifiable approach for designing experiments, particularly before data has been observed: one can use an initial space-filling design to approximate, or emulate, entropy optimal designs for GPs. Subsequently, the initial space-filling design can be sequentially updated to add additional design points using the entropy criterion with an updated estimate of the correlation parameter ρ given the data collected so far.

To illustrate the connection between PPs, space-filling designs, and entropy optimal designs for GPs, the following motivating simulation experiment is considered. For reasons which will shortly become clear, entropy optimal designs for our simplified (stationary, isotropic) GP model will generate point patterns that are stationary and isotropic. When a PP is stationary and isotropic with constant first-order intensity λ_Z , one can use Ripley's K function [[Ripley, 1976](#), [Diggle et al., 2010](#)] to measure spatial dependence in the point patterns, defined to be

$$K_Z(r) = E_Z(r)/\lambda_Z,$$

where $E_Z(r)$ is the expected number of points within a distance of radius r of an arbitrary point. The simulation experiment proceeds by generating 1,000 replicates of entropy optimal designs of size $n = 30$ in $p = 2$ dimensions. Each of these entropy optimal designs is

constructed by starting with a random initial design which is then optimized using the Fedorov Exchange Algorithm for 20,000 iterations. The candidate set of input settings, χ , is taken to be the grid of 50×50 equally spaced points in $[0, 1]^2$. The assumed exponential correlation function is $c(\boldsymbol{\xi}, \boldsymbol{\xi}') = 0.45^{\|\boldsymbol{\xi} - \boldsymbol{\xi}'\|_1}$ where $\|\cdot\|_1$ is the L_1 distance metric. Figure 2 shows the estimated K_Z function [Diggle et al., 2010] averaged over the replicates and 95% pointwise uncertainty intervals for the generated optimal designs as a function of radius r . As a reference, the K_R function for a completely random (Poisson process) point pattern is also shown as the dashed line in the figure. As the estimated K_Z function is less than the K_R function, this indicates evidence of a regular structure to the point pattern [Ripley, 1977, Dixon, 2014].

The evident connection between entropy optimal designs and a regular point pattern is relevant to our goal of emulating designs because of a connection between entropy optimal designs and a particular stochastic process model for a regular PP, which we explore in the next section.

3 Optimal Design Emulator

While the criterion-based view of design introduced in Section 1 is the popular interpretation in the literature, a more formal probabilistic exposition [Kiefer et al., 1985, Müller, 2007] was previously explored. Given such a probabilistic design model, one can imagine our design problem as simply being equivalent to sampling, that is, drawing a realization of a point

pattern distributed according to our model. In the earlier probabilistic exposition from the design literature, this probability model places non-zero weight only on the optimal design points. Formally, we can think of this as a conditional distribution, where the conditionality arises from the criterion function of the design, $\mathcal{L}(\boldsymbol{\xi}_1, \dots, \boldsymbol{\xi}_n)$ achieving a particular value, \mathcal{L}^* , where $\mathcal{L}^* = \min_{\boldsymbol{\xi}_1, \dots, \boldsymbol{\xi}_n} \mathcal{L}(\boldsymbol{\xi}_1, \dots, \boldsymbol{\xi}_n)$.

More broadly, we can cast the design problem as one of needing to define a probability model on any finite collection of points which could make up our design. Unconditionally, we can imagine a corresponding probability model for a fixed cardinality, n , of the resulting point pattern. That is, unconditionally our model will define the probability of all n -run point patterns over the (discrete) sample space χ . The optimal design is one (or a small subset, say, due to isometries) of the point patterns which collectively form the sample space. Denote the stochastic process generating these point patterns by Z , let f_Z represent the probability mass (or density) function of this process, and let $\mathcal{J}(\boldsymbol{\xi}_1, \dots, \boldsymbol{\xi}_n) = \mathcal{M}(\mathcal{L}(\boldsymbol{\xi}_1, \dots, \boldsymbol{\xi}_n))$ for some monotone transformation \mathcal{M} such that \mathcal{J} is a non-negative, Lebesgue-integrable function of the inputs.

Definition: We call the probability model represented by the mass (or density) function f_Z a *design emulator* if $f_Z \propto \mathcal{J}$, where f_Z and \mathcal{J} are defined on the same support χ .

Note that this notion of a design emulator is in terms of the probability representation of a design. In other words, we aim to introduce a statistical model to emulate the probability of the proposed designs. Leveraging this alternative representation, our task will be to arrive

at an appropriate emulator for the probability of design points and to use this model as a means of sampling the optimal design from the stochastic PP Z without resorting to the brute-force optimization techniques that are prevalent in optimal design.

In order to construct a PP-based design emulator for our GP regression model of interest, we are motivated by the so-called *determinantal* PP model from the PP literature, which we introduce in the next section. This model generates point patterns that fall in the regular pattern class of point processes, as introduced in Section 2. Later, we will explore a variant of this model which will motivate a computationally cheap algorithm for emulating the optimal design from our stochastic PP model.

3.1 Determinantal Point Processes

An increasingly popular PP model that generates regular point patterns is the *determinantal point process (DPP)*. The DPP was introduced to the statistics literature only recently [Hough et al., 2006, Kulesza and Taskar, 2011, Lavancier et al., 2014]. It has been applied to sparse variable selection problems [Rocková et al., 2015, Mutsuki and Fumiyasu, 2016] and statistical and machine learning [e.g., Kulesza and Taskar, 2013, Kang, 2013, Affandi et al., 2014, Dupuy and Bach, 2016, Xu et al., 2016].

For entropy optimal designs of GP models, the following result on discrete, finite DPPs due to Kulesza and Taskar [2013] motivates the use of DPP models.

Lemma 1. [Kulesza and Taskar, 2013] For a determinantal point process defined over a

discrete candidate set $\chi \subset \mathbb{R}^d$ with the positive semi-definite kernel function $K(\boldsymbol{\xi}, \boldsymbol{\xi}'; \theta)$ with $\boldsymbol{\xi}, \boldsymbol{\xi}' \in \chi$ and known kernel function parameter θ , the probability mass function for a point pattern realization of cardinality n is given by $f_Z \propto \det(\mathbf{K}_Z)$, where the $n \times n$ positive semi-definite matrix \mathbf{K}_Z has entries $[\mathbf{K}_Z]_{ij} = K(\boldsymbol{\xi}_i, \boldsymbol{\xi}_j; \theta)$.

Based on this result, we immediately have the following.

Corollary. The entropy-optimal design for GP regression model (2) with $\sigma^2 = 1, \sigma_\epsilon^2 = 0$ and correlation function $c(\cdot, \cdot; \rho)$ corresponds to the mode of a determinantal PP with kernel function $K(\boldsymbol{\xi}, \boldsymbol{\xi}'; \theta) \equiv c(\boldsymbol{\xi}, \boldsymbol{\xi}'; \rho)$.

These results provide an elegant connection between entropy optimal designs for GP regression and using DPP models to essentially emulate the point pattern associated with the optimal design by placing a DPP prior on the space of point patterns to which the optimal design belongs. However, on the surface, finding the mode of the DPP is no easier than the usual optimization problem associated with finding the entropy optimal design. A key result, due to [Hough et al. \[2006\]](#), leads to the following approximation to the DPP, known as the *Determinantal Projection Point Process* (DPPP).

Lemma 2. [[Hough et al., 2006](#)] Suppose Z is a DPP with kernel K defined over χ and write $K(\boldsymbol{\xi}, \boldsymbol{\xi}') = \sum_{k=1}^N \lambda_k \phi_k(\boldsymbol{\xi}) \phi_k^T(\boldsymbol{\xi}')$ where ϕ_k 's are orthonormal eigenvectors of K with eigenvalues λ_k ($k = 1, \dots, N$). Define \mathcal{Z} to be a DPPP with kernel given by $\mathcal{K}(\boldsymbol{\xi}, \boldsymbol{\xi}') = \sum_{k=1}^N B_k \phi_k(\boldsymbol{\xi}) \phi_k^T(\boldsymbol{\xi}')$ where the B_k 's follow independent Bernoulli($\lambda_k / (\lambda_k + 1)$) distributions for $k = 1, \dots, N$. Then $\mathcal{Z} \stackrel{d}{=} Z$, where $\stackrel{d}{=}$ denotes equality in distribution.

This result shows that any DPP can be represented as the weighted combination of so-called DPPP's. [Hough et al. \[2006\]](#) show that this result implies a sampling algorithm where one first generates the Bernoulli random variables B_1, \dots, B_N where the number of points in the realization is $n = \sum_{i=1}^N B_i$, and then the locations of the points are generated by (suitably orthonormalized) vectors, whose L_2 norm is interpreted as a discrete probability measure. In other words, sampling from the DPP is simplified by the separation of *how many points* make up a realization and the *location of points* for a realization of a given size; that is

$$\begin{aligned} P(\Xi_n = \{\xi_1, \dots, \xi_n\}, B_1 = b_1, \dots, B_N = b_N) \\ = P(\Xi_n = \{\xi_1, \dots, \xi_n\} | B_1 = b_1, \dots, B_N = b_N) P(B_1 = b_1, \dots, B_N = b_N), \end{aligned}$$

where $n = \sum_{i=1}^N B_i$ is the total number of points appearing in a particular realization.

For our purposes, the generation of point patterns of a random cardinality is not relevant, however the approximation introduced by the DPPP gives us the tools to specify a conditional framework that eventually can be used to give an (approximate) emulator of the entropy optimal design.

3.2 Fixed Rank Determinantal Point Process

[Kulesza and Taskar \[2011\]](#) outline the notion of a fixed-rank DPP, a DPP with a fixed sample size n . That is, the sampling of the B_i 's is conditional on $\sum_{i=1}^N B_i = n$. While technically elegant, their approach is less interpretable from a statistical modeling perspective. In our

approach, we recognize the distribution of B_1, \dots, B_N given $\sum B_i = n$ as a *conditional Bernoulli distribution* [Chen and Liu, 1997]. The advantage of this approach is two-fold. First, we can define a clear hierarchical statistical model for sampling from a fixed-rank DPP. Second, Chen and Liu [1997] provide no less than four algorithms for sampling from this conditional Bernoulli distribution, with differing computational and memory complexity tradeoffs. This allows one to provide a more efficient algorithm for constructing entropy optimal designs.

Conditioning on $\sum B_i = n$, we have the following hierarchical model for the fixed-rank DPP,

$$\begin{aligned} & P\left(\Xi_n = \{\xi_1, \dots, \xi_n\}, B_1 = b_1, \dots, B_N = b_N \mid \sum B_i = n\right) \\ &= P\left(\Xi_n = \{\xi_1, \dots, \xi_n\} \mid \{B_j = 1\}_{j \in \mathcal{S}}, \{B_j = 0\}_{j \in \{1, \dots, N\} \setminus \mathcal{S}}\right) \times \\ & P\left(\{B_j = 1\}_{j \in \mathcal{S}}, \{B_j = 0\}_{j \in \{1, \dots, N\} \setminus \mathcal{S}} \mid \sum_{i=1}^N B_i = n\right), \end{aligned}$$

where \mathcal{S} is the subset of indices of $\{1, \dots, N\}$ of cardinality $|\mathcal{S}| = n$. Calculation of the first term comes from L_2 -norms of appropriate orthonormalizations of the vectors as shown in Algorithm 1. The conditional Bernoulli probability can be calculated sequentially as

$$\begin{aligned} & P\left(\{B_j = 1\}_{j \in \mathcal{S}}, \{B_j = 0\}_{j \in \{1, \dots, N\} \setminus \mathcal{S}} \mid \sum_{i=1}^N B_i = n\right) \\ &= P\left(B_1 = b_1 \mid \sum_{i=1}^N B_i = n\right) \times P\left(B_2 = b_2 \mid B_1 = b_1, \sum_{i=1}^N B_i = n\right) \times \dots \times \\ & P\left(B_N = b_N \mid B_1 = b_1, \dots, B_{N-1} = b_{N-1}, \sum_{i=1}^N B_i = n\right), \end{aligned}$$

using the recursive method of [Chen and Liu \[1997\]](#) which is summarized in the Appendix. Generating a fixed-rank DPP realization using conditional Bernoulli sampling then proceeds similarly as in [\[Hough et al., 2006\]](#), as shown in Algorithm 1. Note that \mathbf{K}_χ denotes the kernel matrix constructed for the candidate set χ .

Algorithm 1: Generating a fixed-rank DPP realization.

```

Input:  $\phi_1, \dots, \phi_N$  and  $\lambda_1, \dots, \lambda_N$  from eigendecomposition of  $\mathbf{K}_\chi = \sum \lambda_i \phi_i \phi_i^T$ 

// Draw from the conditional Bernoulli distribution
Set  $\mathcal{S}_0 = \{\}$  and  $j = 0$ 
Repeat
    Set  $j = j + 1$ 
    Let  $r = |\mathcal{S}_{j-1}|$ .
    With probability  $P(j, r)$  (see Appendix)
        Set  $\mathcal{S}_j = \mathcal{S}_{j-1} \cup j$ 
Until  $|\mathcal{S}_j| = n$ 
Set  $\mathcal{S} = \mathcal{S}_n$ 

// Initialize required quantities given  $\mathcal{S}$ 
Let  $v(\boldsymbol{\xi}) = (\phi_{\mathcal{S}[1]}(\boldsymbol{\xi}), \dots, \phi_{\mathcal{S}[n]}(\boldsymbol{\xi}))^T$ 
Let  $e_j$  be the vector of 0's except 1 in the  $j$ th position,  $j = 1, \dots, n$ 

// Draw the point pattern
for  $j$  in  $n, \dots, 1$ 
    Sample  $\boldsymbol{\xi}_j$  from  $P_j(\boldsymbol{\xi}) = \frac{1}{j} \left( \|v(\boldsymbol{\xi})\|^2 - \sum_{k=1}^{n-j} |e_k^T v(\boldsymbol{\xi})|^2 \right)$ 
    Orthonormalize  $\phi_1, \dots, \phi_{j-1}$  with respect to  $e_j$ 

// Return the drawn fixed rank point pattern realization
return  $\Xi_n = (\boldsymbol{\xi}_1, \dots, \boldsymbol{\xi}_n)^T$ 

```

3.3 Emulating the Optimal Design

Algorithm 1 will generate fixed-rank DPP realizations with a fixed number of points, and while these points should generally exhibit a regular pattern, there is no guarantee that any particular realization would be of especially high quality in terms of the regularity of the point pattern. That is, much like any stochastic process, it is always possible to draw a “bad” realization that has low probability.

Since the entropy optimal design for GP regression corresponds to the mode of a DPP by the corollary to Lemma 1, this suggests taking

$$\Xi_n = \arg \max_{\xi_1, \dots, \xi_n} P(\Xi_n = \{\xi_1, \dots, \xi_n\} | \{B_j = 1\}_{j \in \mathcal{S}^*}, \{B_j = 0\}_{j \in \{1, \dots, N\} \setminus \mathcal{S}^*}),$$

where

$$\mathcal{S}^* = \arg \max_{\mathcal{S}} P\left(\{B_j = 1\}_{j \in \mathcal{S}}, \{B_j = 0\}_{j \in \{1, \dots, N\} \setminus \mathcal{S}} \mid \sum_{i=1}^N B_i = n\right), \quad (4)$$

as our (approximate) emulator of the optimal design.

Theorem 3. The index set given by (4) is $\mathcal{S}^* = \{1, \dots, n\}$.

Algorithm 2: Drawing a fixed rank design from the design emulator.

```

Input:  $\phi_1, \dots, \phi_n$  from the eigendecomposition of  $\mathbf{K}_\chi = \sum \lambda_i \phi_i \phi_i^T$ 

// Initialize required quantities
Let  $v(\boldsymbol{\xi}) = (\phi_1(\boldsymbol{\xi}), \dots, \phi_n(\boldsymbol{\xi}))^T$ 
Let  $e_j$  be the vector of 0's except 1 in the  $j$ th position

// Draw the point pattern
for  $j$  in  $n, \dots, 1$ 
    Set  $\boldsymbol{\xi}_j = \arg \max_{\boldsymbol{\xi}} P_j(\boldsymbol{\xi}) = \frac{1}{j} \left( \|v(\boldsymbol{\xi})\|^2 - \sum_{k=1}^{n-j} |e_k^T v(\boldsymbol{\xi})|^2 \right)$ 
    Orthonormalize  $\phi_1, \dots, \phi_{j-1}$  with respect to  $e_j$ 

// Return design drawn from the entropy optimal design emulator
return  $\Xi_n = (\boldsymbol{\xi}_1, \dots, \boldsymbol{\xi}_n)^T$ 

```

Theorem 3 shows that selecting the set \mathcal{S}^* amounts to calculating the first n (eigenvector, eigenvalue) pairs (i.e. such that $\lambda_1 > \lambda_2 > \dots > \lambda_n$) of the $N \times N$ kernel matrix \mathbf{K}_χ . This eliminates the computational burden of conditional Bernoulli sampling, leading to a fast algorithm for emulating the optimal design. We refer to this fast sampling algorithm for the mode of the fixed-rank DPP as our *optimal design emulator* of entropy designs for GP regression.

The proposed pseudo-code for drawing from the design emulator is shown in Algorithm 2. Note that the inputs to Algorithm 2 depend on the matrix \mathbf{K}_χ having been formed with a “suitable” value of the correlation parameter ρ . As noted earlier, space-fillingness occurs as $\rho \rightarrow 0$ [Mitchell et al., 1994]; in practice we choose a suitably small setting of ρ to construct

space-filling designs using the design emulator.

An example of the design obtained from the design emulator in 2 dimensions is shown in Figure 3 along with 2 random realizations of the fixed-rank DPP drawn according to Algorithm 1 and a design constructed using the space-filling design function `cover.design` of Nychka et al. [2015]. Comparisons in terms of the determinants of the correlation matrices for the resulting designs as well as their runtimes are summarized in Table 1. Since it is typically recommended to perform random restarts of `cover.design` to obtain a solution closer to the global optima, we report the runtime for 0 and 100 restarts. Note that for any random realization of the fixed-rank DPP there is no guarantee that the sampled points will be especially good in terms of space-fillingness; here the two samples drawn seem poor. However, the design emulator results in a design that empirically fills the space well and also produces the best criterion value. At the same time, the design emulator was the fastest of all methods (even using unoptimized R code). While running random restarts of `cover.design` improved the criterion, it also significantly increases the computational cost.

Table 1: Values of the determinant of the correlation matrix for designs resulting from 2 random samples of the fixed-rank DPP, 2 designs generated by `cover.design` using 0 and 100 random restarts, and the emulated optimal design taken as the (approximate) mode of the fixed-rank DPP. The runtimes are indicated in seconds.

| Design Algorithm | random fixed-rank DPP | random fixed-rank DPP | <code>cover.design</code> reps=0 | <code>cover.design</code> reps=100 | design emulator |
|----------------------------------|-----------------------|-----------------------|----------------------------------|------------------------------------|-----------------|
| $\det(\mathbf{R}(\mathbf{E}_n))$ | 2.15e-20 | 2.59e-19 | 1.71e-20 | 2.79e-20 | 5.24e-14 |
| Runtime (s) | 312.0 | 441.5 | 0.521 | 37.76 | 0.169 |

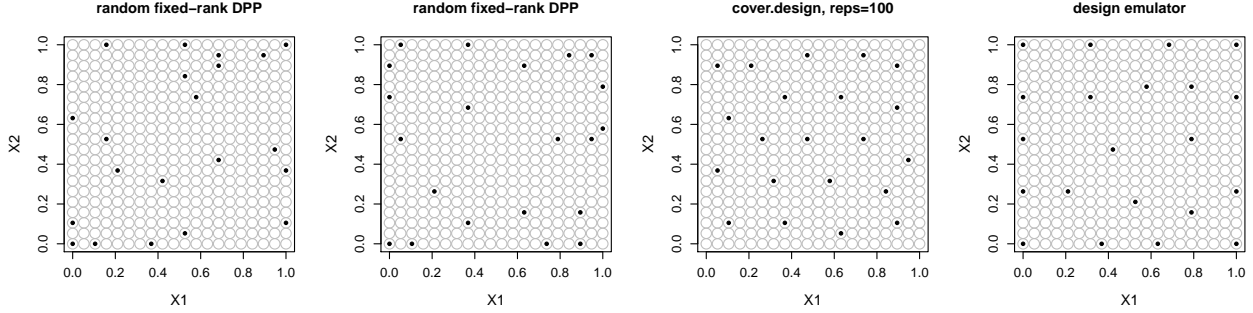


Figure 3: Random realizations drawn from the fixed-rank DPP (left two panels), a space-filling design constructed by 100 random restarts of the `cover.design` function from `R` package `fields`, and the optimal design emulator constructed as the (approximate) mode of the fixed-rank DPP with isotropic Gaussian correlation function in $p = 2$ dimensions with correlation parameter $\rho = 0.01$. All are $n = 21$ point designs.

3.4 Batch Sequential Design via Design Emulator

The design drawn from the design emulator requires specification of the correlation function parameter, ρ , of the GP. Due to the emulator’s speed, it becomes feasible to sample designs for different values of this parameter, or to sequentially update designs with refined estimates of ρ as data are collected. Here we will demonstrate a batch-sequential approach in the case of an isotropic GP.

From Lemma 1, we have that $f_Z \propto \det(\mathbf{K}_Z)$. Suppose an initial design of size n_1 has already been selected consisting of locations $\Xi_1 = (\xi_1, \dots, \xi_{n_1})$ with the corresponding kernel submatrix \mathbf{K}_{Ξ_1} from the overall kernel matrix \mathbf{K}_χ defined on the candidate set χ . Then,

$$f_Z = f_{Z \setminus \Xi_1} \times f_{\Xi_1} \propto \det(\tilde{\mathbf{K}}_{Z \setminus \Xi_1}) \times \det(\mathbf{K}_{\Xi_1})$$

where $\det(\tilde{\mathbf{K}}_{Z \setminus \Xi_1}) = \det(\mathbf{K}_{Z \setminus \Xi_1} - \mathbf{k}_{\Xi_1, Z \setminus \Xi_1}^T \mathbf{K}_{\Xi_1}^{-1} \mathbf{k}_{\Xi_1, Z \setminus \Xi_1})$ denotes the Schur complement of

\mathbf{K}_Z in \mathbf{K}_{Ξ_1} , where $\mathbf{K}_{Z \setminus \Xi_1}$ is the submatrix of \mathbf{K}_Z excluding rows, columns associated with the design points Ξ_1 and $\mathbf{k}_{\Xi_1, Z \setminus \Xi_1}$ is the (rectangular) cross-kernel matrix between design points Ξ_1 and the set of points $Z \setminus \Xi_1$.

The above decomposition allows for a simple sequential updating scheme. Suppose n_a design points Ξ_a have been selected so far (perhaps in a one-shot arrangement, or perhaps as a result of some previous sequential design point selection iterations). To select n_b additional design points, say Ξ_b , one performs the following steps.

1. Construct $\tilde{\mathbf{K}}_{\chi \setminus \Xi_a}$. Note that this matrix assigns probability 0 to (re)selecting any of the first n_a points.
2. Apply Algorithm 2 using the constructed kernel matrix $\tilde{\mathbf{K}}_{\chi \setminus \Xi_a}$. This will sample the next n_b sequential points, Ξ_b , conditional on already having selected the first n_a points.
3. The updated design of $n = n_a + n_b$ points can then be returned as $\Xi_n = \Xi_a \cup \Xi_b$.

The sequential selection steps could then be iterated again to perform further updates.

This conditional approach to sequential design construction is very elegant. We note two situations where application of the approach is useful, and which will be demonstrated in Section 4.2. First, consider sequential designs for GP regression. An initial design would be constructed using a small setting of ρ to emulate a space-filling design. However, in subsequent sequential design updates, data will have been collected giving information on a data-supported value of ρ . At each iteration, the kernel matrix can be updated using the most recent point estimate of ρ , thereby resulting in sequential designs that start off

as space-filling but which evolve to extract more meaningful information from the process being observed:

$$\mathbf{K}_\chi(\cdot, \cdot; \rho_0) \rightarrow \tilde{\mathbf{K}}_{\chi \setminus \Xi_1}(\cdot, \cdot; \rho_1) \rightarrow \tilde{\mathbf{K}}_{\chi \setminus \Xi_1 \cup \Xi_2}(\cdot, \cdot; \rho_2) \rightarrow \dots$$

where the initial “space-filling” value ρ_0 is subsequently updated based on the data collected.

Another relevant scenario is the desire to enforce certain *projection properties* of designs.

Typically, the desired projection property is to enforce space-fillingness or non-collapsingness

in all marginal dimensions as well as in the full d -dimensional design space. For instance, it

is well known that Latin hypercube designs preserve space-fillingness of the 1-dimensional

marginals but do not enforce this constraint on the higher-order marginals. Generally, adding

this constraint to design construction has been a challenge, both in formulating an appropriate

mathematical criterion and in optimizing the resulting criterion. Recently, [Joseph](#)

[et al. \[2015\]](#) proposed a criterion that aims to preserve the space-fillingness constraint in all

marginal sub-spaces when constructing d -dimensional designs, but in general there has been

little work in this area due to the computational difficulty of finding such designs.

Our sequential formulation allows one to easily enforce the non-collapsing projection property

constraint – that is, to remove the possibility of design points overlapping in their marginal

projections. Let

$$S_1 = \{\xi' \in \chi \setminus \Xi \mid \xi'_j = \xi_j \text{ where } \xi \in \Xi \text{ for at least one } j \in 1, \dots, d\},$$

$$S_2 = \{\boldsymbol{\xi}' \in \chi \setminus \Xi \mid \xi'_j = \xi_j \cap \xi'_k = \xi_k \text{ where } \boldsymbol{\xi} \in \Xi \text{ for at least one pair } (j, k) \in 1, \dots, d\},$$

$$S_3 = \{\boldsymbol{\xi}' \in \chi \setminus \Xi \mid \xi'_j = \xi_j \cap \xi'_k = \xi_k \cap \xi'_l = \xi_l$$

$$\text{where } \boldsymbol{\xi} \in \Xi \text{ for at least one tuple } (j, k, l) \in 1, \dots, d\},$$

and so on, where the higher-order sets S_4, \dots, S_{d-1} are similarly defined. Then, it is clearly the case that

$$S_1 \supseteq S_2 \supseteq \dots \supseteq S_{d-1}.$$

Therefore, to find the subset of candidate points that would violate the desired projection constraint in all marginal dimensions, it is sufficient to find the set S_1 alone. Notably, this is an operation that is $\mathcal{O}(Nnd)$ in the worst case (where N is the cardinality of χ , n is the number of design points and d is the dimension of the input space), exhibiting no combinatorial explosion with dimension. Our batch-sequential design algorithm satisfying the non-collapsing constraint is outlined in Algorithm 3.

Algorithm 3: Batch-Sequential Design Emulator with Non-Overlapping Projections.

```

Let  $\Xi_a$  be the  $n_a$  existing  $d$ -dimensional design points  $\xi_1, \dots, \xi_{n_a}$ 
Let  $\chi$  be the original (full) set of candidate points
Initialize  $S = \Xi_a$ 

// Construct the set of points violating the non-collapsing
// projection constraint of the existing design
for  $i$  in  $1, \dots, n_a$ 
    for  $j$  in  $1, \dots, d$ 
        for  $k$  in  $1, \dots, N$ 
            if  $\xi_{ij} == \chi_{kj}$  and  $\chi_k \notin S$ 
                 $S = S \cup \chi_k$ 

// Calculate the conditional kernel matrix
 $\tilde{\mathbf{K}}_{\chi \setminus S} = \mathbf{K}_{\chi \setminus S} - \mathbf{k}_{S, \chi \setminus S}^T \mathbf{K}_S^{-1} \mathbf{k}_{S, \chi \setminus S}$ 

// Draw  $n_b$  batch-sequential points using Algorithm 2 with the
// first  $n_b$  eigenfunctions  $\phi_1, \dots, \phi_{n_b}$  from the eigendecomposition
// of kernel matrix  $\tilde{\mathbf{K}}_{\chi \setminus S} = \sum \lambda_i \phi_i \phi_i^T$ .

```

4 Examples

To motivate the interesting possibilities of using a fast design emulator, we consider a designed variant of the popular Stochastic Gradient Descent (SGD) algorithm as well as sequential designs for GP regression.

4.1 Designed Stochastic Gradient Descent

As mentioned earlier, one motivation for space-filling designs is as a variance-reduction technique when calculating statistical estimators. To demonstrate the potential for a computationally cheap design emulator for constructing space-filling designs in a modern context, we motivate possible modern applications in the big data setting involving the stochastic gradient descent (SGD) algorithm [Bottou, 2010]. SGD is used extensively in statistical machine learning to scale model training to big data for a variety of applications including linear models, clustering, GP regression and deep neural networks [e.g. Zhang, 2004, Sculley, 2010, Dean et al., 2012, Hensman et al., 2013, Wan et al., 2013, Sutskever et al., 2014, Badrinarayanan et al., 2015]. SGD works by using small random subsets of the data, called *batches*, to estimate the gradient. The essential idea of SGD is to sacrifice an increase in estimator variance for computational gain so the parameter space of the model can be more efficiently explored when fitting models to big data. Due to the speed of the proposed design emulator, we can replace SGD’s random subset selection with a space-filling subset selection at each iteration of the algorithm, thereby recovering some of this variance tradeoff.

A small simulation was carried out by generating observations from a 5-dimensional linear regression model (similar to the popular Friedman function [Friedman, 1991]),

$$Y(\mathbf{x}) = \beta_0 + \beta_1 \sin(2\pi x_1 x_2) + \beta_2 (x_3 - 0.5)^2 + \beta_3 (x_4 - 0.5)^2 + \beta_4 x_4 + \beta_5 x_5 + \epsilon, \quad (5)$$

where the regression coefficients β_0, \dots, β_5 were generated as $\text{Unif}(-10, 10)$ and the obser-

| Subset Size | $\frac{\text{MSE}(\hat{\beta}_1 \Xi_R)}{\text{MSE}(\hat{\beta}_1 \Xi)}$ | $\frac{\text{MSE}(\hat{\beta}_2 \Xi_R)}{\text{MSE}(\hat{\beta}_2 \Xi)}$ | $\frac{\text{MSE}(\hat{\beta}_3 \Xi_R)}{\text{MSE}(\hat{\beta}_3 \Xi)}$ | $\frac{\text{MSE}(\hat{\beta}_4 \Xi_R)}{\text{MSE}(\hat{\beta}_4 \Xi)}$ | $\frac{\text{MSE}(\hat{\beta}_5 \Xi_R)}{\text{MSE}(\hat{\beta}_5 \Xi)}$ |
|-------------|---|---|---|---|---|
| | 23 | 1.97 | 1.47 | 1.27 | 2.92 |
| 43 | 1.62 | 1.04 | 1.45 | 2.72 | 1.67 |
| 63 | 1.56 | 0.94 | 2.00 | 2.59 | 1.56 |
| 83 | 1.43 | 1.20 | 1.32 | 2.38 | 1.44 |

Table 2: Ratio of MSE of parameter estimates for random subsets (Ξ_R) versus designed subsets (Ξ) when using SGD to fit the model (5). Values greater than 1.0 indicate the multiplicative factor by which random subsets had larger MSE relative to the designed subsets.

vational error was taken to be $\epsilon \sim N(0, 1)$. The model was fit using SGD with batches of size `batchsize` = {23, 43, 63, 83}. SGD iterates over all the batches of data in random order and repeats this entire process a number of times, called epochs. We used 200 epochs in this example. The total dataset size was $50 \times \text{batchsize}$ and each study was replicated 100 times, using randomly drawn coefficients for each replicate. To evaluate the quality of the SGD solution, we compared the ratio of the average squared error of the regression coefficients for random subsets versus the designed subsets. For example, a ratio of 2 indicates the estimation error was twice as large as that of using SGD with the design emulator.

The results summarized in Table 2 show that even in such a simple example, the resulting error is usually 1.5-3 times worse based solely on how the subsets are selected from the dataset. This demonstrates a novel application of experimental design in the modern big data modeling setting that is enabled by the computationally cheap design emulator.

4.2 Batch-Sequential Designs in GP Regression

Our second demonstration of the proposed technique considers constructing sequential designs for GP regression using Algorithm 3. As outlined in Section 1.1, we assume a stationary GP regression model with mean zero and Gaussian correlation function with no measurement error. First, consider this model in 2 dimensions and look at batch-sequential designs constructed 3-at-a-time and 4-at-a-time, shown in Figure 4. In this figure, the design points are denoted by solid dots and the light gray circles denote available candidate points which, if selected, would negatively impact the space-fillingness of marginal projections. The black circles denote available candidate points that would not negatively impact the marginal projections.

Initial designs were constructed with $n = 3$ (respectively $n = 4$) points and sequentially updated until $n = 9 + 3$ (respectively $n = 12 + 4$). For comparison, the single-shot designs constructed using Algorithm 2 are labelled as $n = 12$ (respectively $n = 16$). The examples shown in Figure 4 show that the sequential approach appears to construct space-filling designs that end up with a similar spread of points as the single-shot design. However, as the projection property is not enforced in this sequence, the marginal projections of the sequential designs are as poor as the single-shot designs. This is easily seen by comparing the number of black circles falling on each marginal dimension for $n = 9 + 3$ versus $n = 12$ and $n = 12 + 4$ versus $n = 16$. In particular, for the 3-at-a-time case, the marginal projections of the sequential and single-shot designs are equally bad.

Next, we consider batch-sequential designs that incorporate the constraint that the marginal

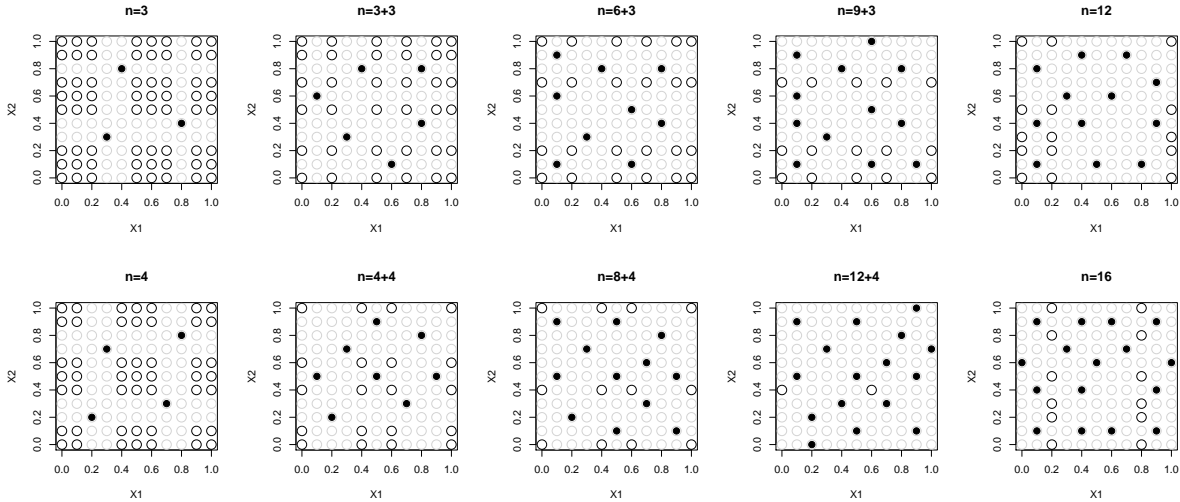


Figure 4: Batch sequential designs. Row 1: batch size of 3. Row 2: batch size of 4. The single-shot designs ($n = 12$ and $n = 16$) are shown in the rightmost column. Solid dots denote designs while empty circles are candidate points. The gray circles denote candidates which would negatively impact the marginal projections. These sequential designs were constructed without regard to the marginal projections.

projections should not overlap as described in Section 3.4. The 3-at-a-time and 4-at-a-time designs are shown in Figure 5. Enforcing this constraint did not have a noticeable computational effect, but the quality of designs is noticeably improved. For instance, the $n = 9 + 3$ design now has only 2 settings in the marginal projections which are unoccupied by design points as compared to the $n = 12$ single-shot design which has 3 and 5 settings of the input dimensions unoccupied by design points. In the 4-at-a-time designs, the $n = 12 + 4$ design has no unoccupied marginal projections while the single-shot $n = 16$ design has 2 and 6 unoccupied marginal projections. These examples demonstrate the efficacy of applying Algorithm 3 to enforce the desired projection properties.

The designs constructed in Figures 4 and 5 use a correlation parameter of $\rho = 1 \times 10^{-10}$ to essentially be constructed as space-filling designs. However, in practice a sequential design

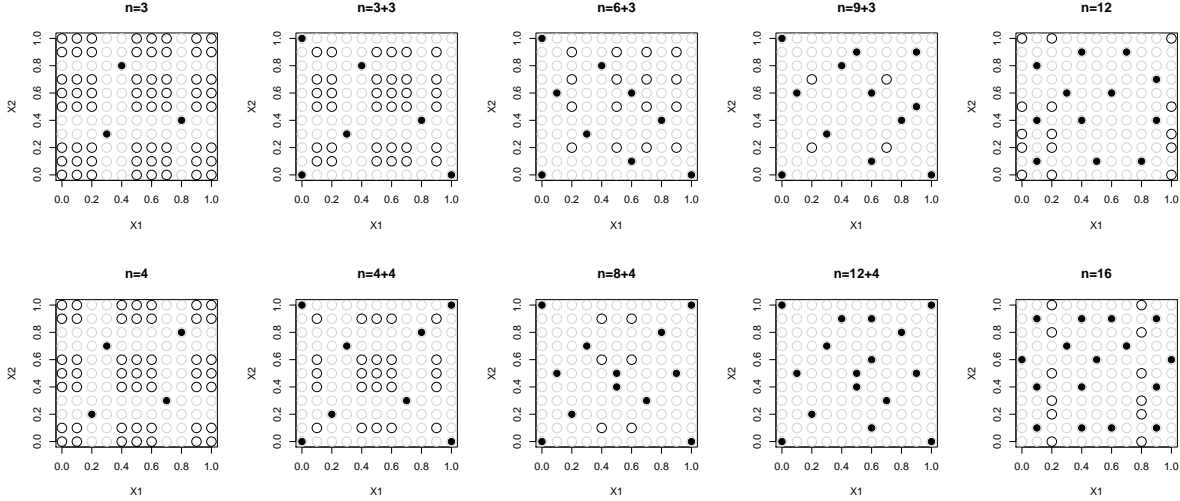


Figure 5: Batch sequential designs with marginal projection constraint. Row 1: batch size of 3. Row 2: batch size of 4. The single-shot designs ($n = 12$ and $n = 16$) are shown in the rightmost column. Solid dots denote designs while empty circles are candidate points. The gray circles denote candidates which would negatively impact the marginal projections. Note how the final sequential designs ($n = 9 + 3$ and $n = 8 + 4$) have few overlapping 1d projections while the single-shot designs ($n = 12$ and $n = 16$) have many.

could benefit from improved estimates of the GP correlation parameter from data collected at each step in the sequence. Using Algorithm 3, we can construct designs which sequentially take this into account, becoming less space-filling while still preserving the desired projection properties. We consider an evolution of ρ over the 4 updates as $\rho = 1 \times 10^{-10} \rightarrow \rho = 1 \times 10^{-5} \rightarrow \rho = 0.001 \rightarrow \rho = 0.001$. The resulting sequential designs are shown in Figure 6. The evolution of both design sequences demonstrate a more centralized pattern to the points as the correlation is updated to represent an observed process that is smooth and slowly varying. Yet, the marginal projection property is still satisfied, with no unoccupied marginal projections for the $n = 9 + 3$ and $n = 12 + 4$ designs as compared to the single-shot designs with $n = 12$ and $n = 16$ runs.

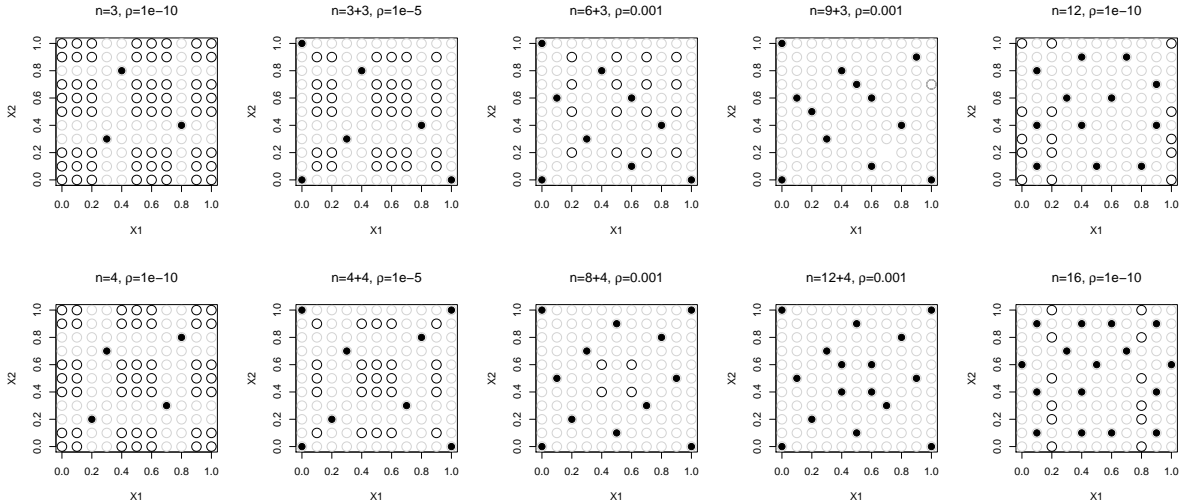


Figure 6: Batch sequential designs with evolving ρ . Row 1: batch size of 3. Row 2: batch size of 4. The single-shot designs ($n = 12$ and $n = 16$) are shown in the rightmost column. Solid dots denote designs while empty circles are candidate points. The gray circles denote candidates which would negatively impact the marginal projections. These sequential designs were constructed to preserve the marginal projection constraint, and assume the correlation parameter is sequentially updated as $\rho = 1 \times 10^{-10} \rightarrow \rho = 1 \times 10^{-5} \rightarrow \rho = 0.001 \rightarrow \rho = 0.001$. The single-shot designs ($n = 12$ and $n = 16$) were constructed using $\rho = 1 \times 10^{-10}$.

5 Discussion

In this article we have introduced a novel probabilistic approach to constructing optimal designs by taking a PP approach. In particular, we considered entropy-optimal designs, which have a clear connection to the popular space-filling designs used in computer experiments and spatial statistics, and we establish their connection to DPPs. By using a discrete version of this representation, we arrive at a computationally efficient algorithm to sample the mode of this PP, which corresponds to the optimal design. Note that our methodology approximately samples the mode of this PP, yet in practice the quality of designs sampled resulted in criterion values many orders of magnitude larger than random DPP samples or

space-filling LHS designs, which implies the approximation is of high quality. Subsequently, we extend the method to allow for sequential design construction and allow one to incorporate a popular marginal projection property constraint without losing the computational benefits of our basic algorithm. Since our approach to enforcing such constraints amounts to specifying a conditional kernel matrix, other constraints not considered in this paper could be easily implemented using the same basic approach described.

The design algorithm introduced in this paper was demonstrated on the popular Stochastic Gradient Descent (SGD) algorithm applied to fitting a model to the popular Friedman test function. SGD works by approximating the model gradient with a small batch sample from the entire dataset and is hugely popular in fitting complex statistical and machine learning models. The algorithm trades off reduced computation time for increased variance in the estimation of the gradients. We have demonstrated that using PPs to select non-uniform, space-filling batches from the design space noticeably improved the performance of the algorithm.

We also demonstrated the sequential variant of our algorithm for GP regression designs that incorporate marginal space-filling projections and/or incorporate updated parameter estimates in a sequential model-fitting exercise. The designs constructed clearly show the effect of incorporating the marginal projection property constraint and the effect of updating the parameter. This allows one to sequentially update the design, starting from a purely space-filling construction when we have not yet observed any information, to one which places greater focus on estimating the model as more data is collected.

Taking inspiration from earlier, and simpler, probabilistic designs in the literature [e.g. [Kiefer et al., 1985](#), [Müller, 2007](#)], this article provides a general approach to constructing designs from a probabilistic PP perspective. While we have focused on designs for stationary GP models, our approach would also apply to non-stationary GP models specified by a closed-form correlation function. The methods outlined in this paper are available on CRAN in the R package `demu`, and we aim to further develop this approach to handle more complex scenarios such as high-dimensional design construction and high-dimensional statistical learning algorithms.

Acknowledgments Peter F. Craigmile is supported in part by the US National Science Foundation (NSF) under grants NSF-DMS-1407604 and NSF-SES-1424481, and the National Cancer Institute of the National Institutes of Health under Award Number R21CA212308. The content is solely the responsibility of the authors and does not necessarily represent the official views of the National Institutes of Health. C. Devon Lin’s research was supported by the Discovery grant from the National Sciences and Engineering Research Council of Canada.

References

- Affandi, R. H., Fox, E. B., Adams, R. P. and Taskar, B. (2014) Learning the parameters of determinantal point process kernels. In *ICML*, 1224–1232.
- Atkinson, A., Donev, A. and Tobias, R. (2007) *Optimum experimental designs, with SAS*. Oxford, UK: Oxford University Press.
- Badrinarayanan, V., Kendall, A. and Cipolla, R. (2015) Segnet: A deep convolutional encoder-decoder architecture for image segmentation. *arXiv preprint arXiv:1511.00561*.

- Banerjee, S., Gelfand, A. E., Finley, A. O. and Sang, H. (2008) Gaussian predictive process models for large spatial datasets. *Journal of the Royal Statistical Society Series B*, **70**, 825–848.
- Bottou, L. (2010) On-line learning for very large datasets. *Proceedings of COMPSTAT'2010*, 177–186.
- Carnell, R. (2016) *lhs: Latin Hypercube Samples*. URL: <https://CRAN.R-project.org/package=lhs>. R package version 0.14.
- Chen, R. B., Hsieh, D. N., Hung, Y. and Wang, W. (2013) Optimizing latin hypercube designs by particle swarm. *Statistics and Computing*, **23**, 663–676.
- Chen, S. X. and Liu, J. S. (1997) Statistical applications of the Poisson-Binomial and conditional Bernoulli distributions. *Statistica Sinica*, **7**, 875–892.
- Cressie, N. and Johannesson, G. (2008) Fixed rank kriging for very large spatial data sets. *Journal of the Royal Statistical Society, Series B*, **70**, 209–226.
- Cressie, N. A. C. (1993) *Statistics for Spatial Data, rev. edn*. New York, New York: John Wiley & Sons Inc.
- Daley, D. J. and Vere-Jones, D. (2003) An introduction to the theory of point processes: volume I: Elementary theory and methods. *Springer-Verlag, New York, New York*.
- Dean, A. M., D. Voss, D. and Draguljic, D. (2017) *Design and Analysis of Experiments, Second Edition*. New York, New York: Springer-Verlag.
- Dean, J., Corrado, G., Monga, R., Chen, K., Devin, M., Mao, M., Ranzato, M., Senior, A., Tucker, P., Yang, K., Le, Q. V. and Ng, A. Y. (2012) Large scale distributed deep networks. In *Advances in Neural Information Processing Systems 25*, 1232–1240.
- Diggle, P. J. (2006) Spatio-temporal point processes: Methods and Applications. *Monographs on Statistics and Applied Probability*, **107**, 1.
- Diggle, P. J., Menezes, R. and Su, T. (2010) Geostatistical inference under preferential sampling. *Journal of the Royal Statistical Society: Series C (Applied Statistics)*, **59**, 191–232.
- Dixon, P. M. (2014) Ripley's k function. *Wiley StatsRef: Statistics Reference Online*.
- Dupuy, C. and Bach, F. (2016) Learning determinantal point processes in sublinear time. *arXiv preprint arXiv:1610.05925*.
- Fedorov, V. V. (1972) *Theory of Optimal Experiments*. New York, New York: Elsevier.
- Friedman, J. H. (1991) Multivariate adaptive regression splines. *The Annals of Statistics*, **19**, 1–67.
- Furrer, R., Genton, M. G. and Nychka, D. (2006) Covariance tapering for interpolation of large spatial datasets. *Journal of Computational and Graphical Statistics*, **15**, 502–523.
- Geyer, C. J. and Møller, J. (1994) Simulation procedures and likelihood inference for spatial point processes. *Scandinavian journal of statistics*, 359–373.
- Gramacy, R. B. and Apley, D. W. (2015) Local gaussian process approximation for large computer experiments. *Journal of Computational and Graphical Statistics*, **24**, 561–578.
- Guhaniyogi, R., Finley, A. O., Banerjee, S. and Gelfand, A. E. (2011) Adaptive Gaussian predictive process models for large spatial datasets. *Environmetrics*, **22**, 997–1007.

- Hensman, J., Fusi, N. and Lawrence, N. D. (2013) Gaussian processes for big data. In *Conference on Uncertainty in Artificial Intelligence*, 282–290. URL: auai.org.
- Higdon, D., Gattiker, J., Williams, B. and Rightley, M. (2008) Computer model calibration using high-dimensional output. *Journal of the American Statistical Association*, **103**, 570–583.
- Hough, J. B., Krishnapur, M., Peres, Y. and B.Virag (2006) Determinantal processes and independence. *Probability Surveys*, **3**, 206–229.
- Johnson, M. E., Moore, L. M. and Ylvisaker, D. (1990) Minimax and maximin distance designs. *Journal of Statistical Planning and Inference*, **26**, 131–148.
- Joseph, V. R., Gul, E. and Ba, S. (2015) Maximum projection designs for computer experiments. *Biometrika*, **102**, 371–380.
- Kang, B. (2013) Fast determinantal point process sampling with application to clustering. In *Advances in Neural Information Processing Systems 26*, vol. 2, 2319–2327.
- Katzfuss, M. (2013) Bayesian nonstationary spatial modeling for very large datasets. *Environmetrics*, **24**, 189–200.
- Katzfuss, M. and Hammerling, D. (2017) Parallel inference for massive distributed spatial data using low-rank models. *Statistics and Computing*, **27**, 363–375.
- Kiefer, J. C., Brown, L. D., Olkin, I. and Sacks, J. (1985) *Jack Carl Kiefer Collected Papers 3: Design of Experiments*. New York, New York: Springer.
- Kulesza, A. and Taskar, B. (2011) k-DPPs: Fixed-size determinantal point processes. *Proceedings of the 28th International Conference on Machine Learning*, 1193–1200.
- (2013) Determinantal point processes for machine learning. *arXiv preprint arXiv:1207.6083*.
- Lavancier, F. and Møller, J. (2015) Modelling aggregation on the large scale and regularity on the small scale in spatial point pattern datasets. *Scandinavian Journal of Statistics*, **43**, 587–609.
- Lavancier, F., Møller, J. and Rubak, E. (2014) Determinantal point process models and statistical inference. *Journal of the Royal Statistical Society: Series B*, **77**, 853–877.
- (2015) Determinantal point process models and statistical inference. *Journal of the Royal Statistical Society: Series B (Statistical Methodology)*, **77**, 853–877.
- Lehmann, E. L. (1966) Some concepts of dependence. *The Annals of Mathematical Statistics*, **37**, 1137–1153.
- Linkletter, C., Bingham, D., Hengartner, N., Higdon, D. and Kenny, Q. Y. (2006) Variable selection for gaussian process models in computer experiments. *Technometrics*, **48**, 478–490.
- McKay, M. D., Beckman, R. J. and Conover, W. J. (1979) A comparison of three methods for selecting values of input variables in the analysis of output from a computer code. *Technometrics*, **42**, 55–61.
- Mitchell, T., Morris, M. and Ylvisaker, D. (1994) Asymptotically optimum experimental designs for prediction of deterministic functions given derivative information. *Journal of Statistical Planning and Inference*, **41**, 377–389.
- Morris, M., Mitchell, T. and Ylvisaker, D. (1993) Bayesian design and analysis of computer experiments: use of derivatives in surface prediction. *Technometrics*, **35**, 243–255.

- Müller, W. G. (2007) *Collecting Spatial Data: Optimum Design Of Experiments For Random Fields, 3rd Edition*. New York, New York: Springer.
- Mutsuki, K. and Fumiyasu, K. (2016) Determinantal point process priors for Bayesian variable selection in linear regression. *Statistica Sinica*, **26**, 97–117.
- Nguyen, H., Craigmile, P. F. and Pratola, M. T. (2019) Near-optimal designs for gaussian process regression models. *submitted*.
- Nychka, D., Furrer, R., Paige, J. and Sain, S. R. (2015) fields: Tools for spatial data. URL: <https://www.image.ucar.edu/fields>. R package version 9.0.
- Pratola, M. T., Chipman, H. A., Gattiker, J. R., Higdon, D. M., McCulloch, R. and Rust, W. N. (2014) Parallel bayesian additive regression trees. *Journal of Computational and Graphical Statistics*, **23**, 830–852.
- Pratola, M. T., Sain, S. R., Bingham, D., Wiltberger, M. and Rigler, J. (2013) Fast sequential computer model calibration of complex spatial-temporal processes. *Technometrics*, **55**, 232–242.
- Ripley, B. D. (1976) The second-order analysis of stationary point processes. *Journal of applied probability*, **13**, 255–266.
- (1977) Modelling spatial patterns. *Journal of the Royal Statistical Society: Series B*, **39**, 172–192.
- Rocková, V., Moran, G. and George, E. I. (2015) Determinantal regularization for ensemble variable selection. *Tech. rep.*, University of Pennsylvania, Philadelphia and 19th International Conference on Artificial Intelligence & Statistics.
- Sacks, J., Welch, W., Mitchell, T. and Wynn, H. (1989) Design and analysis of computer experiments (with discussion). *Statistical Science*, **4**, 409–423.
- Sang, H., Jun, M. and Huang, J. Z. (2011) Covariance approximation for large multivariate spatial data sets with an application to multiple climate model errors. *The Annals of Applied Statistics*, **5**, 2519–2548.
- Sculley, D. (2010) Web-scale k-means clustering. In *Proceedings of the 19th International Conference on World Wide Web*, 1177–1178. ACM.
- Shewry, M. C. and Wynn, H. P. (1987) Maximum entropy sampling. *Journal of Applied Statistics*, **14**, 165–170.
- Silvey, S. D. (1980) *Optimal Design: An Introduction to the Theory for Parameter Estimation*. New York, New York: Chapman & Hall.
- Stein, M. L. (2012) *Interpolation of Spatial Data: Some Theory for Kriging*. New York, New York: Springer.
- Sutskever, I., Vinyals, O. and Le, Q. V. (2014) Sequence to sequence learning with neural networks. In *Advances in Neural Information Processing Systems 27*, 3104–3112.
- Wan, L., Zeiler, M., Zhang, S., Cun, Y. L. and Fergus, R. (2013) Regularization of neural networks using dropconnect. In *Proceedings of the 30th International Conference on Machine Learning (ICML-13)*, 1058–1066.
- Xu, Y., Müller, P. and Telesca, D. (2016) Bayesian inference for latent biologic structure with

determinantal point processes (DPP). *Biometrics*, **72**, 955–964.

Zhang, T. (2004) Solving large scale linear prediction problems using stochastic gradient descent algorithms. In *Proceedings of the Twenty-first International Conference on Machine Learning*, 919–926. ACM.